JOURNAL OF OPTOELECTRONICS AND ADVANCED MATERIALS Vol. 16, No. 5-6, May - June 2014, P. 712 - 718

Investigating the effects of Gamma exposure on the microstructural, optical and track properties of the Pre and Post alpha irradiated PM-355

M. R. BAIG, W. A. FAROOQ*, SYED MANSOOR ALI, TALAL MOHAMMED ALRASHIDI, M. ATIF, S. S. AL-GHAMDI, M. S. ALGARAWI
Department of Physics and Astronomy, College of science P.O box 2455, King Saud University, Saudi Arabia.

In the present investigations, structural and optical variations in PM-355 solid state nuclear track detector are studied at different doses, 20, 40, 60, 80 and 100 kGy of gamma radiation. Effects of gamma radiation on pre and pose alpha irradiated samples of P-355 at the same dose are also studied. Structural and surface variations are studied using XRD patterns and micrographs of scanning microscope. Optical properties are investigated using UV-Vis spectrograph and spectrofluorometer from JASCO. It has been observed that the absorbance of PM-355 material increases with increasing gamma dose and saturated at 60 kGy. Moreover, the variation in the structure and optical properties saturate at 60 kGy of gamma rays. It is also concluded that PM-355 can be good candidate for gamma dosimetry up to 60 kGy radiation.

(Received March 25, 2014; accepted May 15, 2014)

Keywords: Optical properties, Gamma radiation, Charge particles, Photoluminescence.

1. Introduction

PM-355 is a solid state nuclear detector (SSNDT). The chemical composition for PM-355, PM-500 and CR-39 SSNTD detectors are identical: $C_{12}H_{18}O_7$ (polycarbonate of allyldiglycol). The difference among these detectors is the fabrication process[1]. These detectors have many applications. Their application in detection of heavy charged particles and investigation in their structural modification have extensively been reported[2-7]. Among these, PM-355 is excellent in detection of light ions including protons, deuterons, He and C-ions. Due to this property PM-355 is the most appropriate choice for detection application in plasma and typically in laser induced plasma experiments[8, 9]. Their applications in cold fusion, alpha particle and proton detection, neutron dosimetery and radon measurements etc. are reported[10-12].

When heavy charge particles enter in to detector they ionize the detector. The ionization may be very extensive depending on the energy, charge and mass of the ionizing particle and the properties of the detector. The ionizations dissociate the molecules and a series of new chemical processes create free chemical radicals and other chemical species. Cross-linking and chain scission reactions occur between molecules of the detector. During this process if cross-linking reaction is larger than the chain scission, the detector would become hardened, otherwise softening occurs in the detector[13-15]. In the present research we have investigated the effects of gamma exposure on the microstructural, optical and track properties of the Pre and Post alpha irradiated PM-355. The results are useful for the radiation dosimetry.

2. Experimental details

Fifteen samples of PM-355 were used in the present experiment. The samples were divided into three sets .The first set, Set-1 was exposed to gamma beam only with different doses 20, 40, 60, 80 and 100 kGy from Co^{60} source. The second set, Set-2 was first exposed with Gamma source at same doses as Set-1 and then irradiated with alpha for five seconds at a distance of 2cm with Am-241 source (Gamma+alpha). This source emits 5.49 MeV energy alpha radiations. The irradiation process in third set, Set-3 was reversed (alpha+ Gamma) under the same conditions, that is, first all samples were irradiated with alpha at constant dose and then irradiated with gamma, 20, 40, 60, 80 and 100 kGy.

The absorbance spectra of PM-355 were measured with JASCO V-670 UV/Vis Spectrophotometer in the wavelength range of 200-800 nm at room temperature. whereas the fluorescence spectra of PM-355 SSNTDs were obtained with JASCO FP-8200 Spectrofluorometer at room temperature at the excitation wavelength of 250 nm. After obtaining the absorbance spectra the samples of Set-2 and Set-3 were etched under same conditions in 6.25N of NaOH solution at a temperature at 70 ˚C for 3 hrs in order to visualize the tracks. After etching the tracks diameter was measured by an optical microscope (Ziess, Garmany) at a magnification of 400X. The phase crystallinity and structural analysis of the reference and irradiated PM-355 polymers was analyzed by X-ray diffraction patterns using X'pert PRO (PAN analytical) with Cu-K_α source radiation of wavelength of 1.54 Å at

room temperature. The surface morphology before and after irradiation of the PM-355 polymer were analyzed using a Field Effect Scanning Electron Microscope (JEOL FESEM).

3. Results and discussions

Fig. 1 shows the XRD spectra of reference, only gamma exposed and Alpha plus gamma chemically etched PM-355 samples in the range of 2θ between 10 to 80˚. A large bump distributed peak at an angle of 2θ =21.04˚ is observed for reference sample and shifted to 20.36˚ for gamma irradiated sample and 20.29^0 for Alpha plus gamma chemically-etched PM-355, which indicate the amorphous nature of the PM-355 polymer. The shifting of the peak position is due to the stress produced in the material because of ionization process during gamma irradiation. Moreover, the figure shows that the full width at half maximum (FWHM) of this peak become narrower after gamma irradiation and after chemical etching of the PM-355 the FWHM further decreased, which indicate that the crystallite size increased after the gamma irradiation.

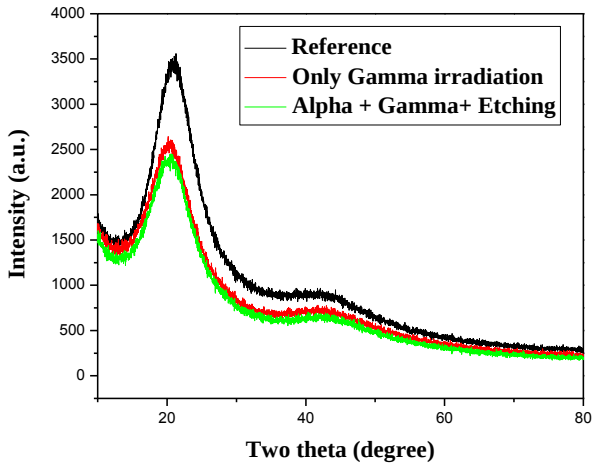

Fig. 1. XRD spectra of reference, gamma irradiated and irradiated plus chemically etched PM-355 SSNTD.

In Fig. 2 (a, b, c) we have presented micrographs of scanning electron microscope (SEM) for reference, only gamma radiated and alpha plus gamma chemically etched samples. Fig. 2 (d) depicts alpha track images of the PM-355 by microscope. It is evident from the Fig. 2 (a) that the grains of reference PM-355 possess spherical-like symmetry in range of 100–170nm with small roughness and after gamma irradiation the spherical grain size increases with large roughness as shown in Fig. 2 (b). Thus SEM studies corroborate the XRD findings, where the crystallite size increases with the gamma irradiation. Fig. 2 (c) is SEM image of Alpha plus gamma radiated chemically etched and Fig 2(d) is Microscopic image of alpha track. The measurements of average diameter of the tracks at different doses are given in table 1.

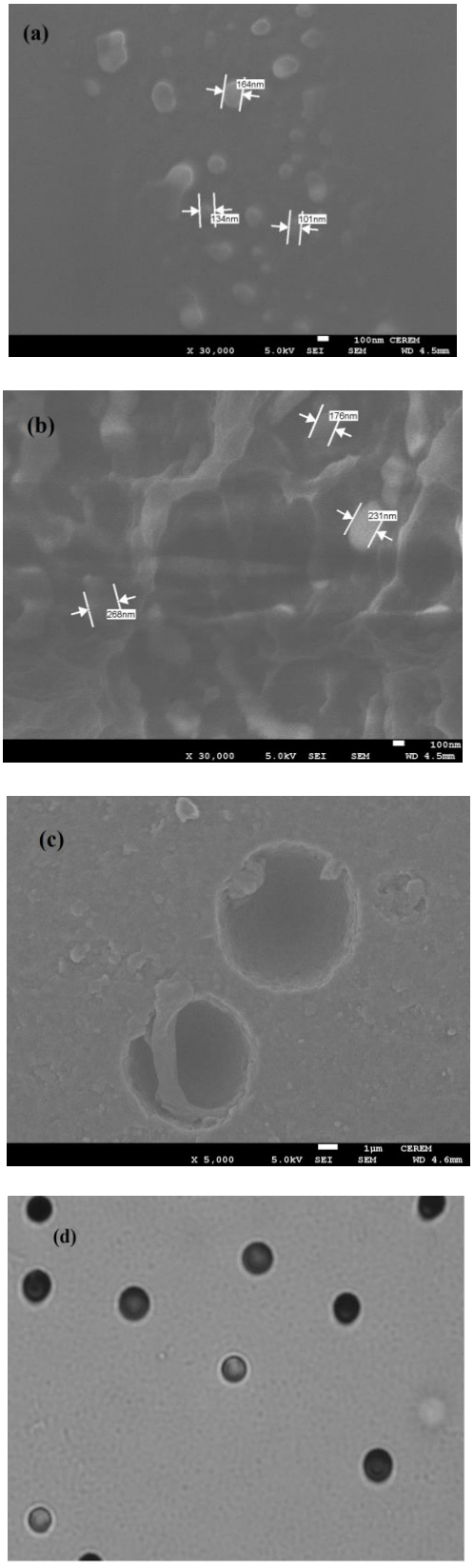

Fig. 2. (a) SEM image of reference (b) SEM image of only gamma irradiated PM-355 (c) SEM image of gamma and alpha irradiated + Chemically etched PM-355 (d) Microscopic image of alpha track.

Table 1. Optical results of all sets at different gamma dose of PM-355 .

Sample Name	Gamma dose (kGy)	Band Gap (eV)					PL Peak Intensity (a.u)					Track Diameter (µm)	
		Set 1	Set 2	Set 3	Set 2 after Etching	Set 3 after Etching	Set 1	Set 2	Set 3	Set 2 after Etching	Set 3 after Etching	Set 2	Set 3
Ref	0	5.5	5.5	5.5	5.46	5.54	50.3	50.3	50.3	50.35	50.35	5.63	5.63
SG1	20	5.42	5.44	5.47	5.29	5.27	48.0	39.3	28.8	136	139.58	8.75	10
SG2	40	5.23	5.26	5.27	4.18	4.27	39.3	33.8	26.3	158.6	156.93	*	*
SG3	60	5.14	5.16	5.19	4	3.81	30.0	32.6	25.6	162	162.97	*	*
SG4	80	5.12	5.11	5.08	3.83	3.65	28.9	31.1	23.8	173.68	164.8	*	*
SG5	100	5.06	5	4.96	3.71	3.61	26.6	19.5	22.0	184	196	*	*

**Irregular shape and very big size track.*

Absorbance spectra of gamma irradiation samples as a function of different doze (Set-1), post alpha irradiation with different gamma doze (Set-2) and pre alpha irradiation with different gamma dose (Set-3) in the range of 225-350 nm are depicted in Fig. 3-(a), (b) and (c) respectively.

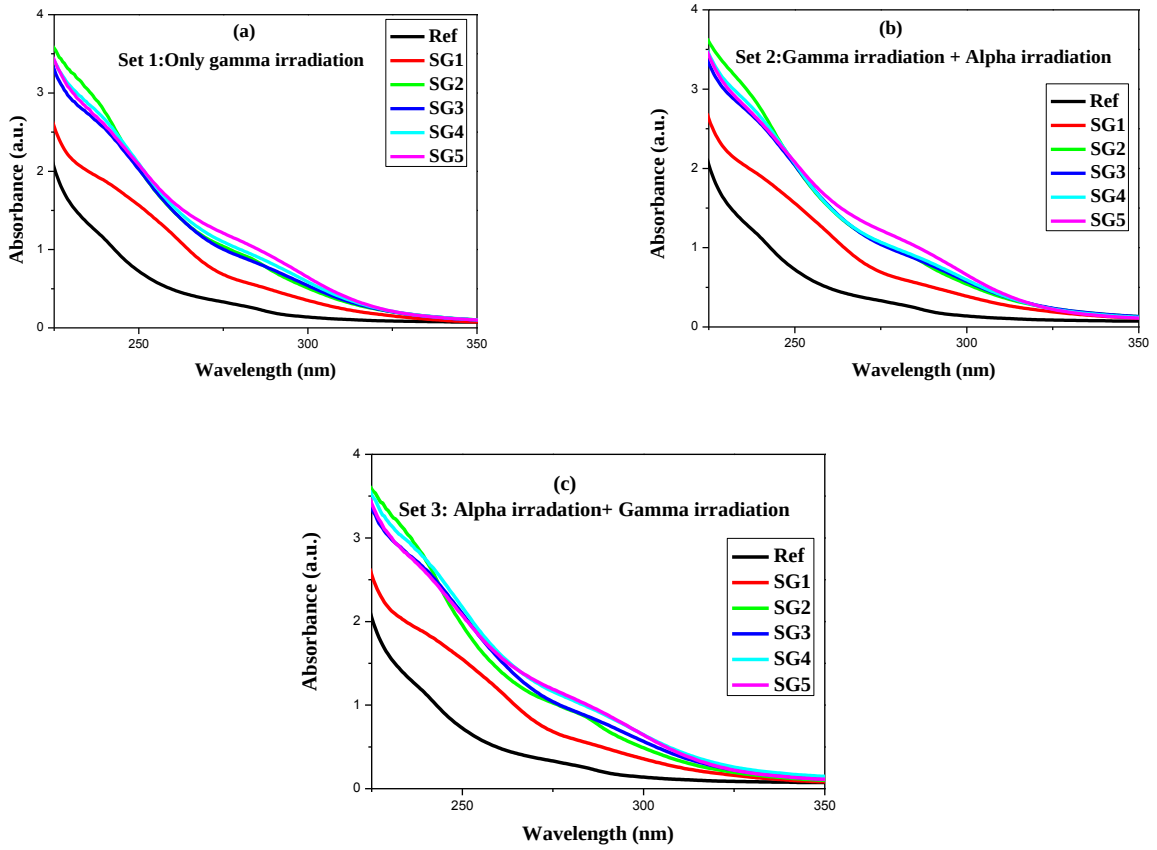

Fig. 3. Absorption spectra (a) for different gamma dose irradiated (b) for post alpha irradiated with different gamma dose (c) for pre alpha irradiation with different gamma dose of PM-533 SSNTDs.

Variation in absorbance as function of gamma dose of three sets show that absorbance increases with increasing gamma dose up to 60 KGy and then further increase in the dose does not increase the absorbance. It means that this is the saturation point in the structure modification with further gamma irradiation [16]. The exposure of gamma radiation induced ionizing in the material which in turn causes the structural defects leading to their density change [17]. After 60 KGy there is no further ionization in the material with increasing gamma ray intensity. It is also observed from fig 3 that absorption edge initially shifted to the longer wavelength upto 60 KGy and then small shift in the absorption edge has been noticed with further increase in dose. It is also due to the saturating in the structural modification of the samples.

In order to measure track diameters due to alpha irradiations on set 2 and set 3, the samples were etched in 6.25N NaOH solution at 70 ^{0}C for three hrs. After etching absorbance of these samples in set-2 and set-3 are measured which are depicted in Fig 4 (a) and (b) respectively. Trend of absorbance variation in these sets is same like before etching but the relative absorbance increases. Comparing the absorbance before and after etching it is concluded that etching does some changes in the structure of this material and widens the tracks diameters.

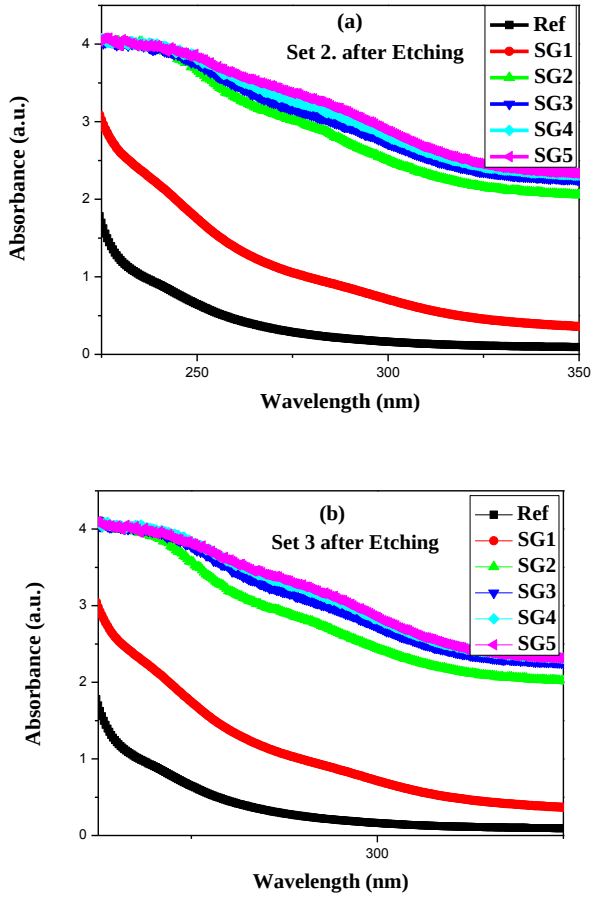

Fig. 4. Absorption spectra of (a) set 2 and (b) set 3 after Etching at 70 ˚C for 3 hrs.

The optical absorption is one of the most important tools to understand the band gap of materials. The optical properties of a solid are governed by the interaction between the solid and the electric field of the electromagnetic wave. To determine optical band gap UV-VIS optical absorption study was carried out on samples after irradiation of samples. The results of optical measurements carried out at room temperature are shown in Fig 3 (a), (b), (c) and Fig 4(a),(b) whereas the optical parameters of these sets are tabulated in Table I. The absorption co-efficient α was calculated from the absorbance

$$\alpha(\lambda) = 2.30At^{-1}$$

Where, t is the sample thickness [18]. In the crystalline and amorphous materials, the optical absorption dependence on the photon energy and it is expressed by the following relationship [18, 19].

$$(\alpha h\nu)^2 = A(h\nu - E_g)^m$$

Where A is an energy independent constant, Eg is the optical band gap and m is a constant to determine the type of optical transition (m = 1/2 and 3/2) for direct allowed and forbidden transitions respectively, m = 2 and m = 3 for indirect allowed and forbidden transitions, respectively. Thus, a more precise value was obtained from the linear part of the $(\alpha h\nu)^2$ vs hν as shown in Fig. 5.

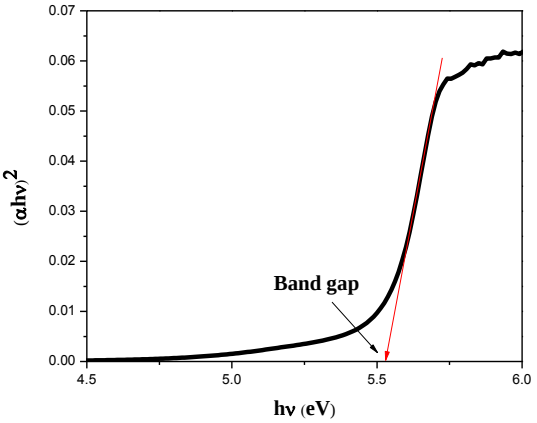

Fig. 5. Calculation of band gap energy.

Variation in Band gap energy with different gamma dose for three sets before etching and Set-2, Set-3 after etching is depicted in Fig 6 and 7 respectively. Fig 6 and Fig 7, show that the band gap decreases as the gamma dose are increased for all the sets. Gamma Irradiation of PM-355 samples leads to chemical changes in polymer chains, i.e cross-linking and chain scission, which all lead to structural modifications and causes variation in optical properties [20, 21, 22]. The inter-particle distance decreased as dose increase, both factors can decrease the band gap of the sample material. In the case of without etching the band gap decrease is almost linear with increasing gamma

dose (fig 6). With etching the trend is different, decrease in band gap is very sharp upto 60 k Gy dose and after that the change is not remarkable. This is also due to saturation in structural modification after 60 k Gy dose.

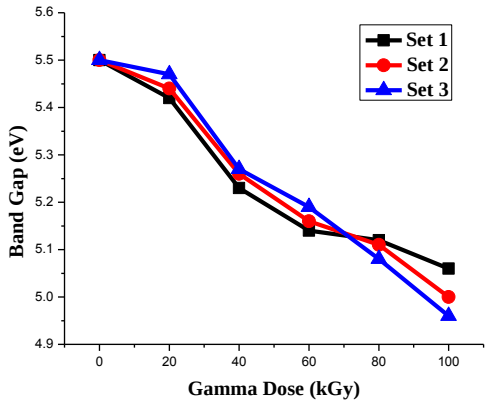

Fig. 6. Variation in Band gap energy with gamma dose for three sets without Etching.

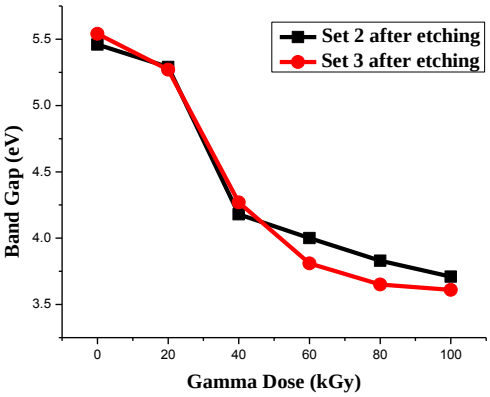

Fig. 7. Variation in Band gap energy with gamma dose set 2 and set 3 after Etching.

The photoluminescence (PL) features of set-1, set-2 and set-3 of PM-355 polymer are scarcely studied. The PL spectra obtained for reference and irradiated samples of set-1, set-2, and set-3 of PM-355 polymer under excitation wavelength of 250 nm are shown in Fig 8(a), (b) and (c) respectively. PL spectra for three sets showed a decrease in the broadband intensity as the dose of gamma radiation is increased. Results are depicted in Fig. 9 and the peaks wavelength are shifted randomly. These changes attribute to the irregular structural change in the samples.

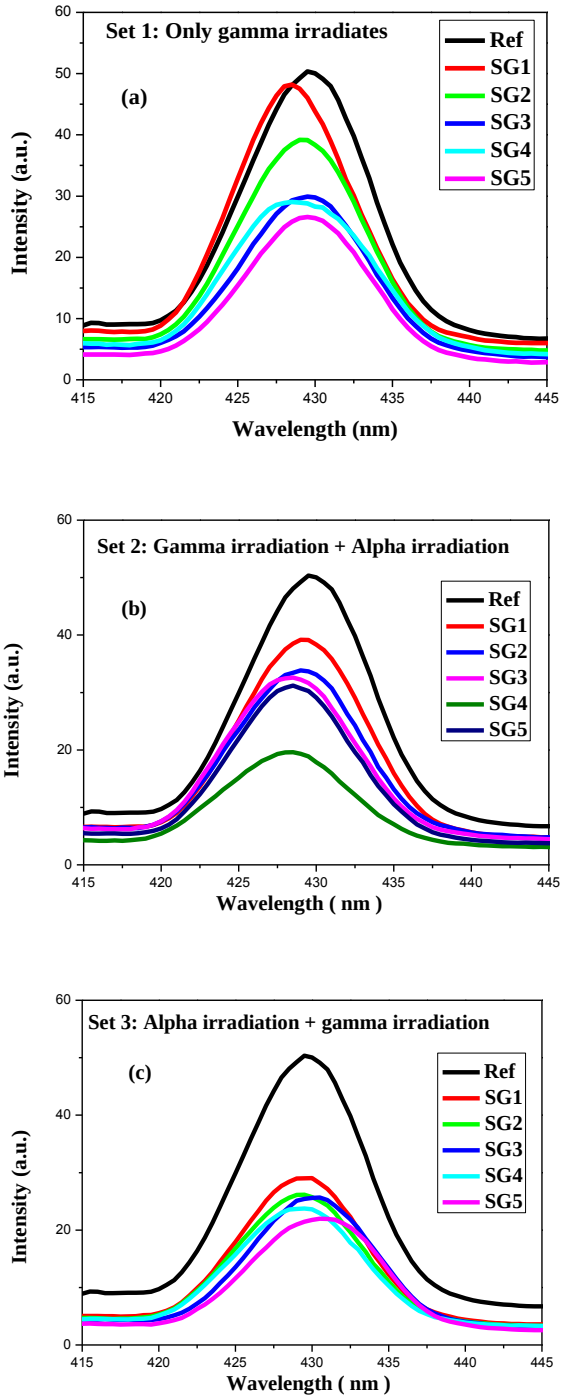

Fig. 8. PL spectra (a) for different gamma dose irradiated (b) for post alpha irradiation with different gamma dose (c) for pre alpha irradiation with different gamma dose of PM-355 SSNTDs.

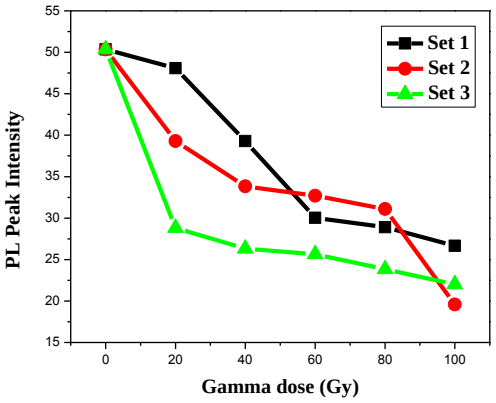

Fig. 9. Variation of PL intensity as a function of different gamma dose for PM-355 SSNTDs without etching.

After etching the photoluminescence spectra of set 2 and set 3 are shown in Fig. 10 (a, b), the PL peak are at the same position and varies with gamma dose randomly but the intensity of the peaks trend are increasing with increasing gamma dose as shown in Fig. 11. This behavior may be due to gamma irradiation induced defects and clusters in the PM-355 polymer which serves as non-radiative centers[23]. The emission bands in the investigated range of wavelength are associated to the less energetic π^*–π and π^*–n electronic transitions[24]. This type of electron transition occurs in the unsaturated centers of the molecules, i.e. in compounds containing multiple (double or triple) bonds, which seems to be more likely process responsible for both increasing and decreasing in the PL intensity.

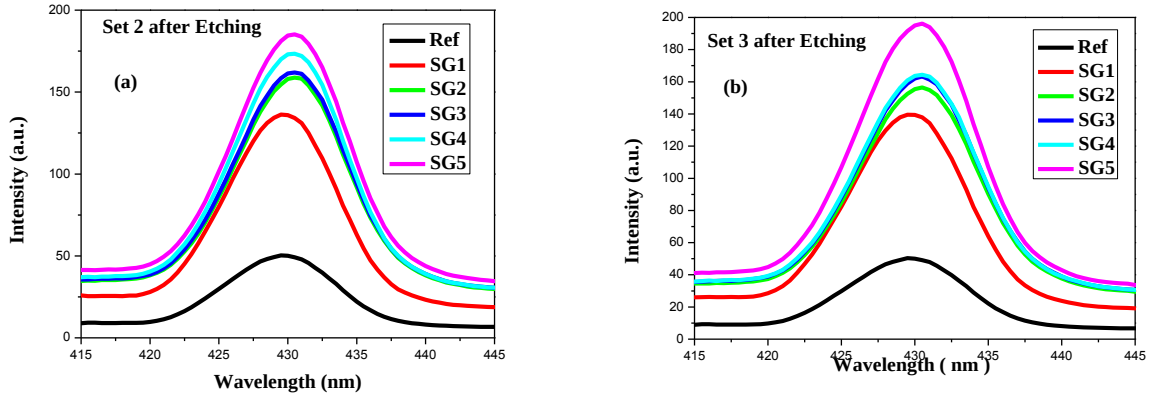

Fig. 10. Absorption spectra of (a) set 2 and (b) set 3 after Etching at 70 ˚C for 3 hrs.

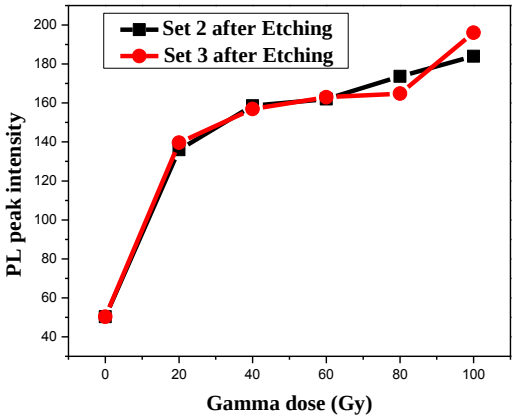

Fig. 11. Variation of PL intensity as a function of different gamma dose for PM-355 SSNTDs after etching.

Variations in track diameters with gamma dose for set-2 and set-3 after chemical etching or irradiated samples are given in Table1. It is also obvious from the data in table-1 that in set-2 samples there is very small effect on Band gap after alpha irradiation.

4. Conclusions

The x-ray diffraction analysis reveals the amorphous nature of the PM-355 polymer. With gamma irradiance full width at half maximum reduces and intensity of peak decreases which indicate that the crystallite size increased after the gamma irradiation. Etching of the samples does not show remarkable change with gamma exposure. Variation in Optical properties is linear up to 60kGy dose and after this dose the variation is not remarkable.

On the basis of the present study, it is evident that PM-355 detectors can be used in gamma dosimetery. It can also be concluded on the basis of this study that UV – visible spectroscopy technique is reliable, repeatable and very useful for identification of effects produced in the structure.

Acknowledgements

The authors would like to extend their sincere appreciation to the Deanship of Scientific Research at King Saud University for its funding of this research through the Research Group Project No. RGP-VPP-293.

References

[1] R. Pugliesi, M. Pereira, M. de-Moraes, M. de-Menezes, App. Rad.and Isotop., **50**, 375 (1999).
[2] M. F. Zaki, E. K. Elmaghraby, J. of Lumin., **132**, 119 (2012).
[3] A. M. Abdul-ader, Basma A. El-Badry, M. F. Zaki, Tarek M. Hegazy, Hany M. Hashem, Philosop. Mag., **90**, 2543 (2010).
[4] A. M. Abdul-Kader, A. Turos, R. M. Radwan, A. M. Kelanyl, Appl. Surf. Sci., **255**, 7786 (2009).
[5] A. M. Abdul-Kader, A. Turos, R. M. Radwan, A. M. Kelanyl, Appl. Surf. Sci., **255**, 5016 (2009).
[6] B. A. El-Badry, M. F. Zaki, A. M. Abdul-Kader, Tarek M. Hegazy, A. Ahmed Morsy, Vac., **83**, 1138 (2009).
[7] B. A. El-Badry, M. F. Zaki, Tarek M. Hegazy, A. Ahmed Morsy, Radiation Effects & Defects in Solids, **163**, 821(2008).
[8] A. Szydlowski, Rad. Measure. , **36**, 35 (2003).
[9] A. Szydlowski, J. Badziak, J. Fuchs, M. Kubkowska, P. Parys, M. Rosinski, R. Suchanska, J. Wolowski, P. Antici, A. Mancic, Rad. Measure., **44**, 881 (2009).
[10] J. E. Groetz, A. Lacourt, P. Meyer, M. Fromm, A. Chambaudet, J. Potter, Rad. Protect. Dos., **85**, 447 (1999).
[11] A. S. Roussetski, Application of CR-39 Plastic Track Detector for Detection of DD and DT-Reaction Products in Cold Fusion Experiments' in 8th International Conference on Cold Fusion, Lerici (La Spezia), Italy: Italian Physical Society, Bologna, Italy, 2000.
[12] R. Banjanac, A. Dragić, B. Grabež, D. Joković, D. Markushev, B. Panić, V. Udoviči, I. Aničin, Phy. Chem. and Tech., **4**, 93 (2006).
[13] D. A. Young, Nature, **182**, 375 (1958).
[14] E. C. H Silk, R. S Barnes, Philos Mag., **4**, 970 (1959).
[15] S. M. A. Durrani, F. Abu-Jarad, Nucl. Instr. and Meth., **100**, 97 (1995).
[16] N. E. IPE, Radiat. Prot. Dosim., SLAC-PUB-3800, **14**, 237 (1986).
[17] R. Y. Zhu, Accelerators, Spectrometers, Detectors and associated equipment, **413**, 279 (1998).
[18] J. Tauc, Amorphous and Liquid Semiconductors, Plenum Press, London and New York, p. 159, 1974.
[19] M. Fox, Optical Properties of Solids, Oxford University Press, Inc., New York., 2001.
[20] H. S. Virk, A.K. Srivastava, Radiat. Measur., **34**, 65 (2001).
[21] T. Steckenreitera, E. Balanzat, H. Fuess and C. Trautmann, Nuclear Instruments Methods Phys. Res. Sect. B: Beam Interac. Mater. Atoms, **131**, 159 (1997).
[22] R. Singh, K. S. Samra, R. Kumar, L. Singh, Radiat. Phys. Chem., **77**, 575 (2008).
[23] R. A. M. Rizk, A. M. Abdul-Kader, Z. I. Ali, M. Ali, Vacuum, **83**, 805 (2008).
[24] A. Douglas Skoog, M. Donald West, Principles of instrumental analysis. 2nd ed. Philadelphia, PA: Saunders College, 1980.

*Corresponding author email: wafarooq@hotmail.com